

**Illuminating snow droughts: The future of Western
United States snowpack in the SPEAR large ensemble**

Julian Schmitt¹, Kai-Chih Tseng²³⁴, Mimi Hughes⁵, Nathaniel Johnson²

¹Harvard University

²Geophysical Fluid Dynamics Laboratory

³Princeton University

⁴Department of Atmospheric Sciences, National Taiwan University, 10617, Taipei, Taiwan

⁵Earth System Research Laboratories/ Physical Sciences Laboratory

Key Points:

- Driven largely by the last two decades, western U.S. severe snow droughts have increased in frequency by 40-50% across all major watersheds over the last 60 years.
- The SPEAR climate model accurately simulates the rapid acceleration of western U.S. severe snow drought occurrence that began in the early 2000s.
- SPEAR projects that increasing temperatures will cause the West to transition to a no-snow environment by the end of the 21st century.

Abstract

Seasonal snowpack in the Western United States (WUS) is crucial for meeting summer hydrological demands, reducing the intensity and frequency of wildfires, and supporting snow-tourism economies. While the frequency and severity of snow drought is expected to increase under continued global warming, quantifying both the response of snow drought to radiative forcing and uncertainties from internal climate variability provides a significant challenge. To evaluate projected changes in WUS snow droughts and their uncertainty, we analyzed a 30-member large ensemble global climate model with moderately high atmospheric resolution ($\sim 50\text{km}$), the Seamless System for Prediction and Earth System Research (SPEAR). To monitor changes in WUS snow droughts in both an observational dataset and SPEAR, we developed a non-parametric drought classification scheme for monthly snowpack. We find that SPEAR predicts dramatic increases in snow droughts, with a 8.8-fold increase under the SSP5-8.5 emissions pathway and a 5.2-fold increase under SSP2-4.5 by 2100. These changes are primarily driven by an increase in monthly temperature anomalies and not a decrease in precipitation. To assess summer water availability we define a condition called "no-snow" which measures when a location has on average less than 10% of its historical April snowpack for the previous 10-year period. After aggregating to the regional level, we found large variability in onset times of no-snow conditions, attributable to internal climate variability. Across the SSP5-8.5 30-member ensemble spread, SPEAR projects that California, for example, could experience no-snow conditions across 90% of the historically snowy region as early as 2058 or as late as 2096. Such a wide range emphasizes large irreducible uncertainty from internal atmospheric variability on WUS snow drought. This uncertainty has large implications for the regions water management and habitability over the coming century.

Plain Language Summary

When winter snow on the ground is significantly less than normal, a region is said to experience a snow drought. Recently, the Western United States has seen a sharp uptick in the frequency of severe snow droughts. As the region depends on stored mountain snowpack, snow droughts have amplified water shortages and wildfires. Here, we use a new climate model to examine snow drought projections through 2100. We find that under a high emission scenario, they could become 9 times more frequent by 2100. Using a large ensemble model, we also examine how internal climate variability impacts how soon regions reach a state of "no-snow" in April. California, for example, reaches no-snow conditions anywhere from 2058 to 2096 under the high emissions scenario. This variability has implications for Western water management and habitability over the coming century.

1 Introduction

Mountains in the Western United States (WUS) have been coined the "water towers" of the West, storing winter precipitation as snow and releasing it during the dry spring and summer as meltwater to populations which have increasingly high water needs (Barnett et al., 2005). Alongside direct benefits of sustained snowpack to human water needs, several indirect benefits such as reduced forest fires (Trujillo et al., 2012; Gergel et al., 2017) and improved snow tourism economics, makes snowpack essential to the WUS' environment and its people. Low or variable snowpack means the opposite: decreased water security, increased fire season activity, and unpredictable snow conditions for tourism (Wobus et al., 2017). Despite large variability from season to season, climate change is already having a measurably significant impact on WUS snowpack, moving towards decreasing snowpack, particularly in late winter (Barnett et al., 2005; Huning & AghaKouchak, 2020). When snowpack, or snow-water equivalent (SWE - the depth of water if all snow melted

66 instantaneously), levels fall significantly below normal, the region is said to experience
 67 a snow drought. Snow drought affects the WUS' economy and human activities, includ-
 68 ing areas far from mountain snowpack which rely on spring and summer meltwaters for
 69 crop production and human consumption.

70 While hydrological drought has immediate impacts on water resources and avail-
 71 ability, the impact of snow droughts (SDs) is typically not felt until summer when early
 72 or low snowmelt can exacerbate meteorological drought. Mountains play a key role in
 73 WUS water supply, as their lower temperatures and higher precipitation capture signif-
 74 icant water reserves in the form of snowpack. Dry WUS summers make the region re-
 75 liant on a steady supply of melting water throughout much of the spring and summer.
 76 Winters with low snowpack typically exacerbating water shortages and increasing wild-
 77 fire frequency and intensity (Barnett et al., 2005; Trujillo et al., 2012; Gergel et al., 2017).
 78 Snow droughts come in two types: dry and warm, which have different hydrologic effects.
 79 Dry snow droughts occur when low precipitation, but normal or cold temperatures, re-
 80 sults in low stream flow during the melt season. Warm snow droughts are characterized
 81 by normal precipitation but high temperatures and usually have rapid early season snowmelt
 82 resulting in increased reservoir flood risk in early spring, followed by drought conditions
 83 as mountain SWE is quickly depleted (Harpold et al., 2017). Shrestha et al. (2021) have
 84 shown that there is a critical threshold of -6 to -5°C for average winter temperatures above
 85 which additional warming begins to significantly decrease snowpack. All 5 WUS water-
 86 sheds fall into this category, and so we expect its snowpack is vulnerable to any level of
 87 warming (Shrestha et al., 2021).

88 Previous literature has shown that large observational uncertainty in climatolog-
 89 ical SWE remains across the WUS. Observational uncertainty is particularly high in re-
 90 gions with complex terrain and low sampling rates, such as mountains, as temperature
 91 and precipitation uncertainties are magnified in snowfall estimates. Coupled global cli-
 92 mate models (GCMs) face similar challenges but to a greater degree because they must
 93 also simulate temperature and precipitation, and are without access to the high-resolution
 94 of a variable infiltration capacity (VIC) model, which is needed to accurately resolve snow-
 95 pack over complex mountain terrain (McCrory et al., 2017; Kim et al., 2021; Wrzesien
 96 et al., 2019; McCrary et al., 2022). Despite large biases and variability in simulating cli-
 97 matological SWE, these models exhibit more uniformity in simulating robust decreases
 98 in WUS SWE (Matiu & Hanzer, 2022). Recently Huning and AghaKouchak (2020) have
 99 shown that SD total duration, average duration, and intensity in the WUS has increased
 100 by 28% between 1980 and 2018, while Shrestha et al. (2021) finds that conditions are
 101 expected to continue to worsen because of the WUS' low latitude. As a result, we will
 102 primarily focus on comparing changes in SWE across data sets.

103 To investigate historical and future changes in SD frequency and intensity we use
 104 a 30-member initial condition state-of-the-art coupled large ensemble global climate model,
 105 called the Seamless System for Prediction and EArth System Research Large Ensem-
 106 ble (hereafter SPEAR). We first show SPEAR accurately simulates changes in WUS se-
 107 vere snow drought (D2+ SD) by comparing to an observational dataset and with pre-
 108 vious studies across the historical period (1921-2011) (Livneh et al., 2013; Huning & AghaK-
 109 ouchak, 2020). Here, the D2+ SD classification includes all snow droughts in the severe,
 110 extreme, and exceptional (D2, D3, and D4) drought categories as described by the US
 111 Drought Monitor (Svoboda et al., 2002). We then explore the magnitude of the projected
 112 changes by assessing the proportion of months that experience D2+ SD, looking both
 113 at the ensemble mean across the WUS through time alongside the ensemble member path-
 114 ways. To determine what is driving the rapid acceleration in D2+ SD frequency, we de-
 115 compose drought conditions by their temperature and precipitation anomaly what con-
 116 ditions are driving these changes. We then provide a watershed-level assessment of the
 117 probability of a “no-snow” environment by the end of the century that explicitly accounts
 118 for both scenario uncertainty and internal climate variability.

By separating the uncertainty into the portion attributable to internal climate variability and emissions uncertainty we can determine the distribution of D2+ SD changes over the next 80 years, variability in the conditions which generate drought/non-drought conditions, and the probability distribution of the transition timing to a no-snow regime. To verify that SPEAR accurately reconstructs changes, we first look over the historical period (1921-2014), which includes observed time-varying natural and anthropogenic radiative forcing, and then consider future projections (2014-2100) under a middle-of-the-road (Shared Socioeconomic Pathway 2-4.5, hereafter SSP2-4.5) and a high emissions scenario (SSP5-8.5) (Delworth et al., 2020). While the two emissions scenarios allow us to explore the effects of emissions uncertainty, SPEAR's 30-member ensemble provides an estimate of internal climate variability.

2 Data and Methods

2.1 SPEAR Large Ensemble Global Climate Model

To assess historical and future changes in snow drought, we analyzed snow water equivalent (SWE) across the Western United States from the 30-member **S**eamless **S**ystem for **P**rediction and **E**Arth system **R**esearch large ensemble (hereafter SPEAR) (Delworth et al., 2020). SPEAR is a coupled global climate model recently developed at the NOAA Geophysical Fluid Dynamics Laboratory (GFDL) that is designed for improved prediction on seasonal to decadal timescales. SPEAR comprises GFDL's AM4 atmosphere, LM4 land, MOM6 ocean, and SIS2 sea-ice models. These component models are the same as GFDL's Global Climate Model version 4 (CM4, Held19), which is a contributor to the Coupled Model Intercomparison Project, phase 6 (CMIP6), but SPEAR's configuration and physical parameterization choices are optimized for climate prediction and projection from seasonal to centennial timescales. SPEAR has moderately high resolution in the atmosphere and land (50 km resolution) and a coarser ocean and sea ice horizontal resolution of about 1° which telescopes to 0.33° meridional spacing near the equator. For this study, we use SPEAR's monthly SWE, temperature, and precipitation across the historical period, from 1921-2014, and projections from 2014-2100 under both SSP2-4.5 and SSP5-8.5 emissions scenarios.

2.2 Observational Data

To evaluate SPEAR's historical simulation of SWE, temperature, and precipitation we use an observations-based dataset (Livneh et al., 2013), available from 1915 to 2011, hereafter the Livneh dataset. Livneh is statistically gridded from in situ observations of precipitation and temperature to 1/16° resolution, and contains daily temperature, precipitation observations, plus SWE estimates which are generated using the VIC land model. To compare with the SPEAR ensemble members, we re-gridded Livneh to SPEAR's 1/2° grid and re-sampled to SPEAR's monthly timescale. Despite incorporating observational data, SWE has perennially been hard to constrain (Wrzesien et al., 2019). Many recent papers have found SWE estimates to vary widely, upwards of a factor of 3 in some cases (Wrzesien et al., 2019) leading us to expect significant absolute biases between SWE estimates (McCrary et al., 2017, 2022). To overcome this issue, we focus our analysis on proportional changes, comparing SWE values to their own historical distributions within each dataset, and then comparing these relative changes across datasets.

We chose 1921-2011 as our historical period as it is the overlapping period of the Livneh and historical SPEAR datasets. This window provides 90 complete winters (91 years) which we use to validate SPEAR and to develop a baseline to which we compare the modeled future climatology. We chose to consider data at monthly resolution intervals for three reasons: (1) data availability, as SPEAR only recorded SWE at monthly intervals, (2) consistency with previous studies, as other papers have done similar anal-

ysis (Huning & AghaKouchak, 2020), and (3) monthly resolution is an appropriate timescale for monitoring snow drought.

2.3 Comparison of a Climate Ensemble to Observations

Several previous studies validate SPEAR against historical conditions. Maher et al. (2022) assesses Pacific Decadal Oscillation (PDO) teleconnections to temperature and precipitation patterns across North America by validating observational data against 5 large ensembles, including SPEAR. They find that SPEAR has both low bias in representing PDO, particularly along the US West Coast. In addition to the assessment in Delworth et al. (2020), which finds minimal temperature and a slight precipitation biases, this study further validates SPEAR as accurately reproducing atmospheric conditions across WUS. As both studies have shown SPEAR to well-represent atmospheric conditions across the WUS, we focused our validation on WUS SWE. We first compare SPEAR ensemble members to the Livneh dataset over the historical period. As Livneh contains a single realization of the historical period, e.g. what actually happened, while the SPEAR ensemble runs capture many possible historical climates, we do not expect the Livneh measurement to align with the SPEAR ensemble mean because changes to the ensemble mean represent the radiatively forced component of the climate with internal variability filtered out. The internal variability is an essential component of individual realizations, contributing significantly to inter-model spread in CMIP multi-model ensembles (Deser et al., 2020) and is essential for modeling extremes. However, we do expect SPEAR to simulate a realization of the climate at least as extreme as the observed historical climate over most regions, although with only 30 members it's still reasonable to expect some observations may fall outside of the SPEAR spread. Thus, if the change in snow drought frequency observed in Livneh falls within the SPEAR ensemble spread, we can assume SPEAR produces a realistic historical climate. We hope the Livneh statistics will fall near the majority of SPEAR ensemble members, as this will further strengthen the conclusion that SPEAR accurately represents WUS climate.

2.4 Drought Classification

Before we can assess changes in snow drought measurements, we must first define snow drought. We base our definition on the historical distribution of SWE by gridcell and month. We restrict our region of study to the “historically snowy” region, areas that historically have seasonal snowpack maxima that average above 20mm SWE, based on the SPEAR ensemble mean. This ensures only regions that typically have snow are eligible for classification.

Our methodology assigns standardized indices to each location by month and uses the US Drought Monitor’s drought classification method for hydrological drought to categorize observations into descriptive bins; near normal, abnormally dry, and moderate, severe, extreme, and exceptional drought, see Figure S1 (Svoboda et al., 2002; Huning & AghaKouchak, 2020). We use a non-parametric empirical model to classify SWE, temperature, and precipitation values for each month. Without assuming the underlying distributions, a non-parametric model allows us to efficiently capture the variability without imposing subjective constraints on the data. It also allows us to compare drought frequency and severity across different hydrological regions and datasets.

We begin by assigning each winter month of the year (Oct-April) a score based on the historical conditions at that location. Our time indices are by year (y) and month (m), e.g. $t_{1931,1}$ for January, 1931, and spatial indices are at intervals of 0.5 degrees of latitude (i) and longitude (j). Thus $s_{40,250}^{t_{1931,1}}$ corresponds to a SWE value at latitude-longitude pair (40, 250) during January 1931. We now compute an empirical distribution over $S_{i,j}^m = (s_{i,j}^{t_{1921,m}}, s_{i,j}^{t_{1922,m}}, \dots, s_{i,j}^{t_{2011,m}})$, representing the historical SWE values during month m at location (i, j) . We then assign a value in $(0, 1)$ to each SWE measurement using the empirical cumulative distribution function, $\hat{F}_{i,j}^m$, based on the proportion of the observed

data in $\mathbf{S}_{i,j}^m$ that fall below it. In equation 1, \mathbb{I} represents an element-wise indicator for each element of $\mathbf{S}_{i,j}^m$ being below x and N represents the total number of measurements, in this case $2011 - 1921 = 90$.

$$\hat{F}_{i,j}^m(x) = \frac{\text{no. of SWE values less than } x}{N} = \frac{1}{N} \sum_{l=1}^N \mathbb{I}(\mathbf{S}_{i,j}^m < x) \quad (1)$$

For each observed or simulated SWE value, $s_{i,j}^{t,y,m}$, we can then compute the z-score by plugging the SWE value into the corresponding \hat{F} and then into the inverse normal distribution, Φ . We refer to these scores as ZSWE, which are indexed by location, month, and year. We can now classify snow droughts from the SWE value, $s_{i,j}^{t,y,m}$, using

$$ZSWE_{i,j}^{y,m} = \Phi\left(\hat{F}_{i,j}^m(s_{i,j}^{y,m})\right) \quad (2)$$

Each month is then assigned either a drought severity label, D0-D4, NN for “near-normal” conditions, or W0-W4 for increasingly wet months. See Table S1 for the full classification scheme and probability of occurrence. While we primarily use this framework to classify snow droughts, we extend the methodology to temperature and precipitation classification as needed. A similar empirically derived methodology is used by Huning and AghaKouchak (2020) to classify snow droughts across the Alps, Himalayas, and Western United States. More generally, this framework is inspired by the US Drought Monitor which uses the same D0-D4 classification. Their classification scheme, however, is not purely statistical, instead relying on experts for the final say on local drought classification. As we cannot rely on experts, our model attempts to match the frequency of meteorological droughts in the US Drought Monitor with snow drought frequency. While our method may result in a mismatch of SWE values and impact in some locations, it provides a statistical way to quickly capture extremes without gathering detailed human and environmental data for each pixel.

2.5 Computing Changes in Snow Drought

We can now apply our drought classification scheme to evaluate how well SPEAR reconstructs historical changes. We define two 41-year windows containing 40 complete winters to assess change over, and after applying our drought classification scheme we count the number of D2+ SD occurrences across the early and late historical, given by a ZSWE of less than -1.3 , e.g. $\mathbb{I}(Z_R^t < -1.3)$ for region R at time t . The percent change for a given region, Δ_R , is derived via

$$\Delta_R = \frac{\sum_{t'} \mathbb{I}(Z_R^{t'} < -1.3)}{\sum_t \mathbb{I}(Z_R^t < -1.3)} \quad \text{for } t \in (1930, 1970), \quad t' \in (1971, 2011) \quad (3)$$

For example, in the Upper Colorado region Livneh observes 27 months of D2+ SD in the early historical period and 28 in the late historical period, translating to an increase of 3.7%. We leverage the SPEAR ensemble spread below to determine whether the overall trend is significant.

2.6 Snow Transition Threshold

In addition to evaluating drought climatology, we are also motivated to determine how a changing snowpack will affect water resources. We want to determine when a shifting climate will begin to severely and persistently impact snow as a water resource. Long-term droughts are particularly damaging, as one or two years of low snow-pack can be buffered by groundwater, above-ground reservoirs, or stored in live biomass, but these buffers dwindle with extended exposure to drought conditions. Thus, we are particularly

interested in determining when no-snowpack is expected to become systemic (Siirila-Woodburn et al., 2021).

Understanding the fraction of snow that remains in a typical year is important for water management (Harpold et al., 2017). To assess this threat, we focus on the fraction of April SWE that remains in historically snowy regions across each of the 5 HUC2 watersheds. We classify an April ($m = 4$) grid cell $s_{i,j}^{t,4}$ as no-snow (or snow free) for that year if there is *at most* 10% of the historical snowfall average remaining at the location (Siirila-Woodburn et al., 2021). We then calculate the regional no-snow area proportion as the fraction of the historically snowy region which experiences those conditions. We let \mathcal{N}_R^Y to denote this no-snow area proportion, where R represents the region, and Y the year. As before, $S_{i,j}^{t_Y,4}$ is the average historical SWE value for the grid cell and $s_{i,j}^{t_Y,4}$ the SWE value for the specific year. Using 10% as our snow free threshold, $\mathcal{T} = 0.1$, then \mathcal{N}_R^Y can be written as:

$$\mathcal{N}_R^Y = \frac{\sum_{(i,j) \in R} \mathbb{I}(s_{i,j}^{t_Y,4} < \mathcal{T} \cdot S_{i,j}^{t_Y,4})}{|(i,j) \in R|}. \quad (4)$$

Thus we have a fraction of the historically snowy region that is snow free in a given year in April. To assess when no-snow conditions become endemic, we apply a 10 year moving-window mean and then define the no-snow transition time as the year when the moving-window mean *last* crosses the area threshold, \mathcal{A} , before 2100. Applying this procedure to all ensemble members, we compute a distribution for when these conditions are likely to become endemic. Formally, the no-snow transition time, \mathcal{T} , is given by:

$$\mathcal{T} := \left[\min t : \tilde{\mathcal{N}}_R^{t'} \geq \mathcal{A} \forall t < t' \leq 2100 \right]. \quad (5)$$

Where $\tilde{\mathcal{N}}_R^{t'}$ gives the moving-window mean fraction of region R that experiences no-snow conditions at time t' . By requiring the moving-window average to be above \mathcal{A} for all subsequent years (until 2100), \mathcal{T} is uniquely determined. For a graphical explanation of this method, please refer to Figure S4.

249 3 Results

250 3.1 SPEAR Model Evaluation

251 3.1.1 SPEAR Ensemble Mean Bias

252 We begin our evaluation with a brief comparison of Livneh and SPEAR winter mean
 253 SWE. We do this by averaging over the winter season, Oct-April, for the period of dataset
 254 overlap, 1921-2011. We find that SPEAR has a negative snow bias across much of the
 255 Mountain West, see Figure 1. In particular, regions characterized by high elevation of-
 256 ten have SWE values over 100% higher in the Livneh dataset than SPEAR. However,
 257 this is not particularly surprising as resampling the 1/16° Livneh grid to match SPEAR's
 258 1/2° grid introduces bias as higher elevations have disproportionately more snow as com-
 259 pared with elevation (McCrary et al., 2022). However, despite these large absolute bi-
 260 ases, we can still use SPEAR to quantify future snow droughts if it reasonably reproduc-
 261 es trends and relative variability in SWE, temperature, and precipitation. To make these
 262 comparisons we leverage the distribution of the SPEAR large ensemble, allowing us to
 263 create a distribution of potential historical outcomes, to compare against the Livneh dataset.
 264 We also compare historical temperature and precipitation changes in Figure S1. Precip-
 265 itation biases are consistently high across much of the Western US as seen in Figure 1
 266 – these findings are consistent with Delworth et al. (2020).

267 3.1.2 Evaluating Snow Drought Changes across the Historical Period

268 When examining historical changes, we find that SPEAR historical snow drought
 269 and temperature trends are already significant, based on a 95% confidence interval for

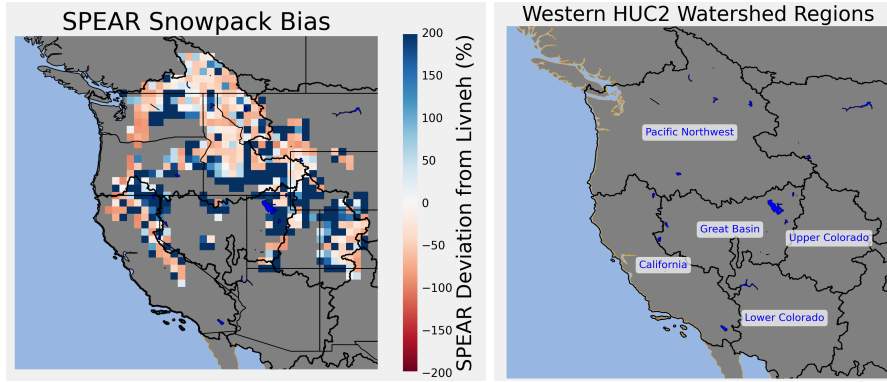


Figure 1. SPEAR winter (Oct-Apr) (a) snowpack (%) and (b) map of the 5 study HUC2 regions of interest.

| Historical Changes in Snow Drought Frequency by Region (%) | | | | | |
|------------------------------------------------------------|-----------------|--------------------|-------------------|----------------------|--|
| HUC2 Region | Livneh Increase | SPEAR Avg Increase | SPEAR Mean 95% CI | SPEAR Ensemble Range | |
| Upper Colorado | 4 | 53 | [30, 77] | [-50, 236] | |
| Lower Colorado | 14 | 26 | [13, 40] | [-39, 107] | |
| Great Basin | 45 | 48 | [26, 70] | [-40, 225] | |
| Pacific Northwest | -55 | 43 | [16, 71] | [-68, 255] | |
| California | 9 | 46 | [25, 67] | [-34, 192] | |

Figure 2. Summary table of Livneh and SPEAR average D2+ SD frequency changes for each of the 5 Western HUC2 regions. Changes are measured between the early (1930-1970) and late (1971-2011) historical periods. As SPEAR is a large ensemble we include a 95% confidence interval which assumes normally distributed changes, and a range of changes across the ensemble.

the ensemble mean assuming an underlying normal distribution in changes. Changes in SWE across all 5 studied HUC2 regions, the Upper Colorado, Lower Colorado, Great Basin, Pacific Northwest, and California regions (abbreviated UC, LC, GB, PNW, and CA) show with ensemble means ranging from 26% (LC) to 53% (UC) increases in D2+ SD occurrence, as in Table 2. The Livneh dataset always falls within the ensemble spread (Table 2), although it is not always in the ensemble mean 95% CI. We present the distribution of D2+ SDs across the historical period (1980-2011) for SPEAR ensemble members, the SPEAR mean, and confidence interval, along with the Livneh observation in Figure 3. These results were consistent with findings in Huning and AghaKouchak (2020), who use 1980-2018 as their historical period — in fact, the 95% confidence interval for the SPEAR ensemble mean across 4 of the 5 regions contains the 28% benchmark for drought intensity increases found in Huning and AghaKouchak (2020), with only the UC interval exceeding the benchmark with a 30% lower bound on historical D2+ SD increases. While we were unable to use an identical historical period due to data constraints, the agreement helps to further validate the SPEAR ensemble. See supplemental Text S1 and Figure S3 for an analysis of changes in precipitation and temperature across the historical period.

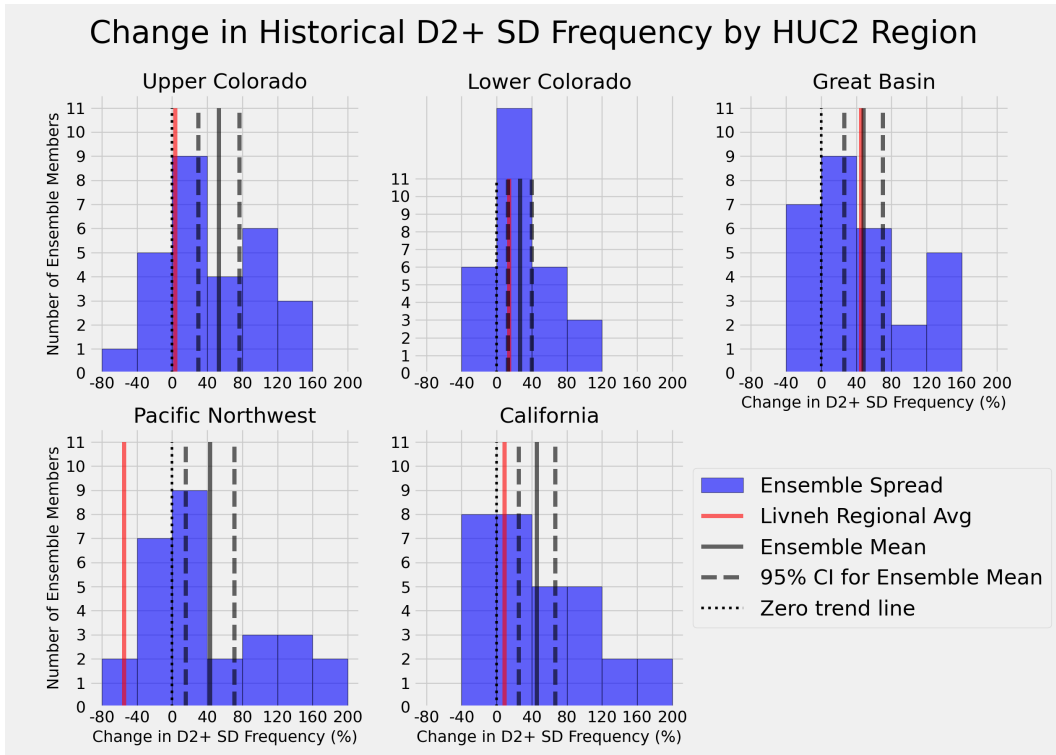


Figure 3. Comparison of SPEAR estimated D2+ SD increases across the historical to Livneh observed increases. The SPEAR distribution is given by the histogram in blue, with the red vertical line representing the observed change in the Livneh dataset. The solid and dashed gray lines represent the mean and 95% confidence interval for each region's ensemble mean, while the dotted line represents the zero trend line.

287 **3.2 Analyzing Snowpack into the 21st Century: Accelerating Loss**

288 We next shift our attention to projected changes in 21st century D2+ SD, focusing
 289 first on changes in droughts classified with our ZSWE metric. We construct our em-
 290 pirical CDF $\hat{F}_{i,j}^m$ distributions from the historical period (1921-2011) and calculate cor-
 291 responding ZSWE scores for each winter month across the historically snowy west 2014-
 292 2100 for all 30 ensemble members. Projected changes in snowpack are dramatic, with
 293 rapid increases in D2+ SD occurring at mid-century (Figure 4). Under SSP5-8.5, we find
 294 that towards the end of the century, all regions are projected to experience severe, ex-
 295 treme, or exceptional drought during most months. Under SSP2-4.5, snow drought in-
 296 creases are less severe, with conditions by the end of the century resembling conditions
 297 under SSP5-8.5 by mid-century. As expected, the higher forcing scenario corresponds
 298 with accelerated increases in snow drought frequency. Snow drought frequencies for all
 299 18 study decades are shown in Figure S4.

300 Examining the distribution of D2+ SDs spatially in Figure 4, a pattern of regional
 301 “hot-spots” emerge. D2+ SD frequency is consistently higher in certain regions begin-
 302 ning in 2030. For example the Washington Cascades and Colorado Rockies are predicted
 303 to experience more frequent snow drought occurrences across all decades than regions
 304 in south-central Idaho and the California Sierra Nevada. We expected to see more dra-
 305 matic D2+ SD increases in the Southern Basins, California and the Lower Colorado, as
 306 they are most susceptible to warming, as even low amounts of warming at southern lat-
 307 itudes results in strong loss signals (Shrestha et al., 2021). We hypothesize that we are
 308 looking over a narrow enough range of latitudes that the latitude signal is overshadowed
 309 by regional variation, perhaps coming from elevation variability. Shrestha et al. (2021)
 310 looked at basins ranging from the Yukon to Columbia river basins that have average win-
 311 ter temperatures of -8°C to +4°C, finding that below -5°C to -6°C warming temperatures
 312 didn’t reduce snowpack. Our HUC2 regions had mean winter temperatures in histori-
 313 cally snowy regions ranging from -5.1°C (UC) to 0.3°C (California), and so we expect
 314 that any warming will produce decreases in snowpack, and corresponding increases in
 315 D2+ SD occurrence.

316 While Figure 4 demonstrates the expected impacts of increasing greenhouse gases
 317 over the next century, as captured by the ensemble mean, it does not indicate how in-
 318 ternal climate variability may exacerbate or alleviate the radiatively forced changes. As
 319 regions must be prepared for conditions less favorable than an ensemble mean, the SPEAR
 320 large ensemble allows us to quantify the uncertainty of these ensemble mean changes that
 321 is attributable to internal variability by looking across the ensemble spread. By aggre-
 322 gating snow drought counts to the entire WUS, and then looking at changes for individ-
 323 ual ensemble members, we can visualize changes in ensemble snow drought through time
 324 (Figure 5).

325 Figure 5 shows the percentage of months by decade which experience D2+ SD in
 326 each of the SPEAR ensemble members. We find that members experience 5-12% D2+
 327 SD frequency in the historical period, averaging 6.5% between 1920 and 2000. Under SSP5-
 328 8.5 this likelihood increases to over 35% snow drought frequency by 2050. Under SSP2-
 329 4.5, the same conditions are reached in 2070. We note the SSP5-8.5 curve is initially flat
 330 until 2000, where snow drought occurrence starts increasing and continues to grow unchecked;
 331 under SSP2-4.5 the curve has a second inflection point at 2070, where the increase in snow
 332 droughts flattens significantly. Interestingly, we note that Livneh does not observe the
 333 same uptick in drought frequency in 2000 where it diverges from SPEAR. However, when
 334 examining the observed changes in Figure 3, we see that there is a significant decrease
 335 in D2+ SD frequency in the Pacific Northwest. The region saw a 54% decrease in snow
 336 drought. This decrease, while in the SPEAR ensemble range, is far from the SPEAR en-
 337 semble mean and perhaps explains the deviation.

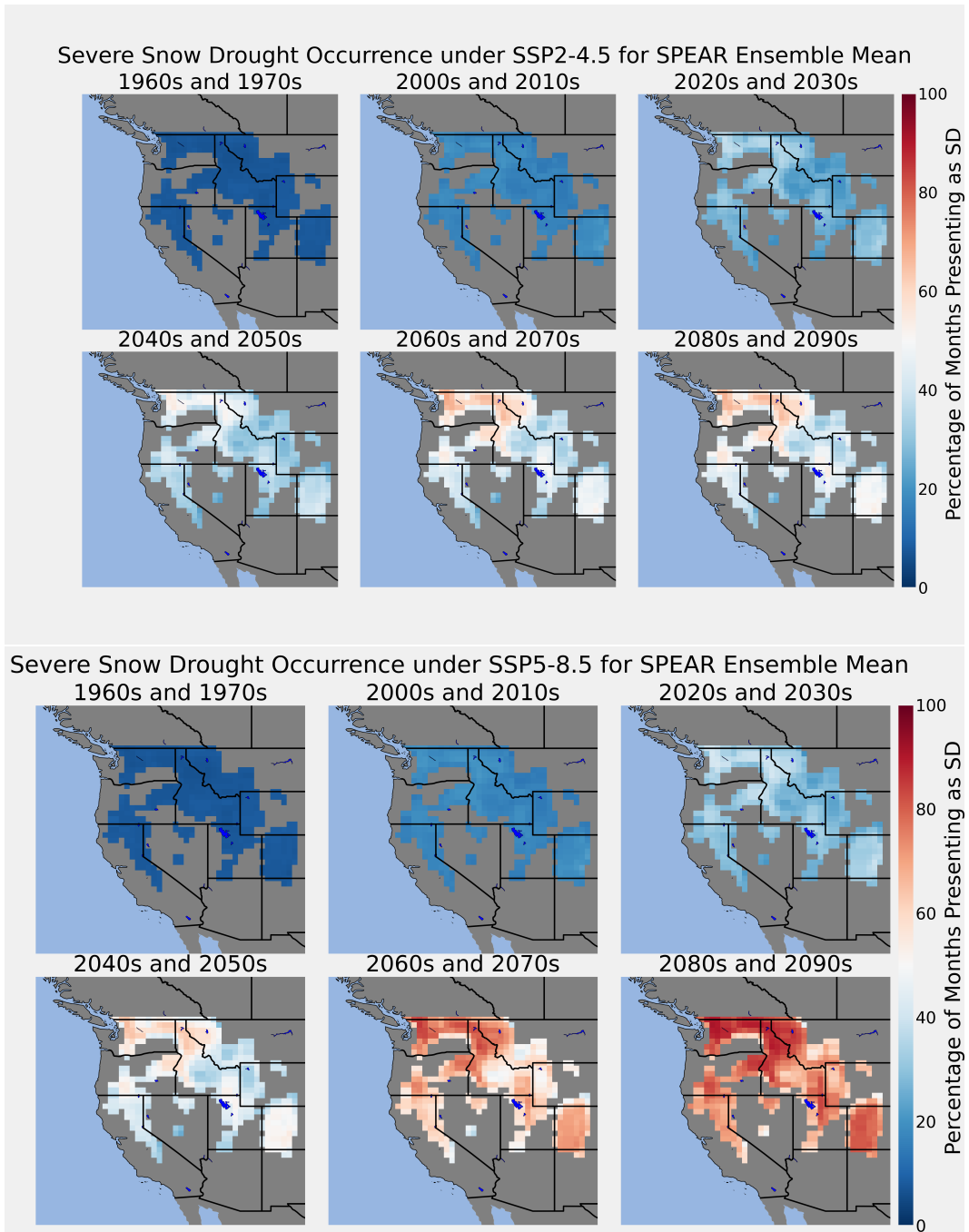


Figure 4. SPEAR snow drought changes highlighted from 1960-2100 under low (SSP2-4.5) and high (SSP5-8.5) emissions scenarios. The plots are masked to historically snowy regions which are colored by the percentage of winter months that the grid-cell experiences snow drought grouped every 2 decades. Historically snowy regions are characterized by having an average peak SWE of at least 20mm.

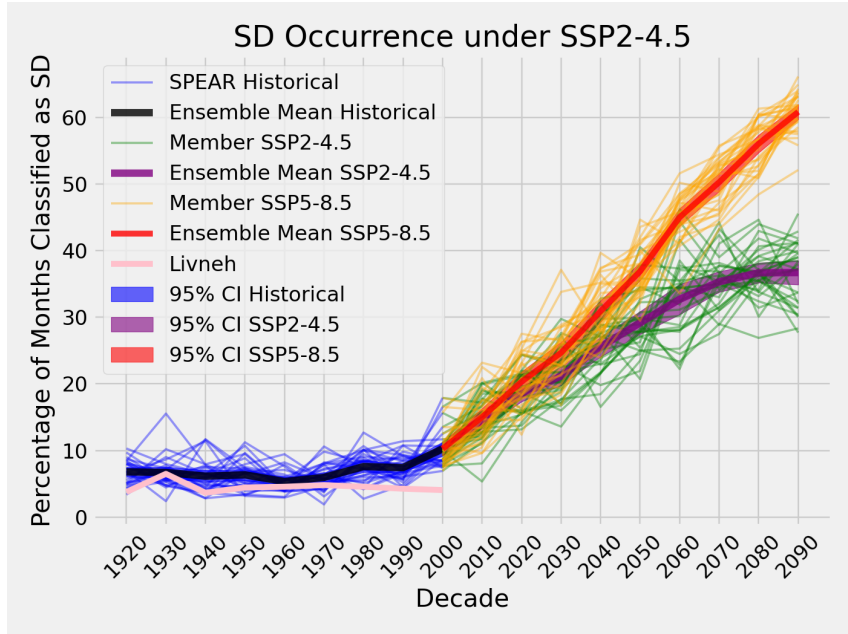


Figure 5. Decadal average of the number of SD months per grid cell. The green trend curves represent the ensemble mean averages for the historical and RCP 4.5 scenarios, while the orange curves depict the RCP 8.5 scenario. Ensemble mean and error is shaded darker.

338 3.3 Temperature and Precipitation Controls on SWE

339 As changes in SWE are primarily driven by changes in temperature and precipi-
 340 tation climatology (McCrory et al., 2017; Harpold et al., 2017), we next examine changes
 341 in SWE in the phase space spanned by temperature and precipitation. By aggregating
 342 over the entire historically snowy Western United States, we can determine how tem-
 343 perature and precipitation anomalies are driving the dramatic increase of droughts. In
 344 Figure 6, each dot represents the average temperature and precipitation anomaly by decade
 345 and is colored according to the average ZSWE score. By definition, the average all-month
 346 historical (1921–2011) temperature and precipitation mean is $(0, 0)$. However, by break-
 347 ing the century down by decade we can see variation within the 20th century.

348 As expected, all-month decadal averages in the historical period cluster around zero
 349 temperature and precipitation deviation, and move as the underlying temperature and
 350 precipitation climatology shifts. In general we see small changes in anomalies between
 351 decades before 2000 which are consistent with our understanding of changing D2+ SD
 352 frequency. Beginning with the 2000s, the decadal averages for the all-month condition
 353 rapidly shift towards warmer and wetter conditions. For example, by 2050 under SSP5-
 354 8.5, the average temperature and precipitation are 1.50 and 0.25 standard deviations higher
 355 than the 20th century average, respectively. This corresponds to a dramatic warming and
 356 slight wetting across the WUS, and indicates that we expect the average month in 2050
 357 to be warmer than 93% of months in the historical period for a given location. For SSP2-
 358 4.5, the values are 1.18 and 0.20, respectively, reflecting a still moderate increase in tem-
 359 perature and precipitation by mid-century, with the average month in 2050 being warmer
 360 than 88% of historical months.

361 To investigate how droughts specifically are changing, we also tracked just the months
 362 which experienced D2+ SD to see how the average drought month has changed (outlined
 363 in grey in Figure 6). We find that historical D2+ SD averages are both dry and warm

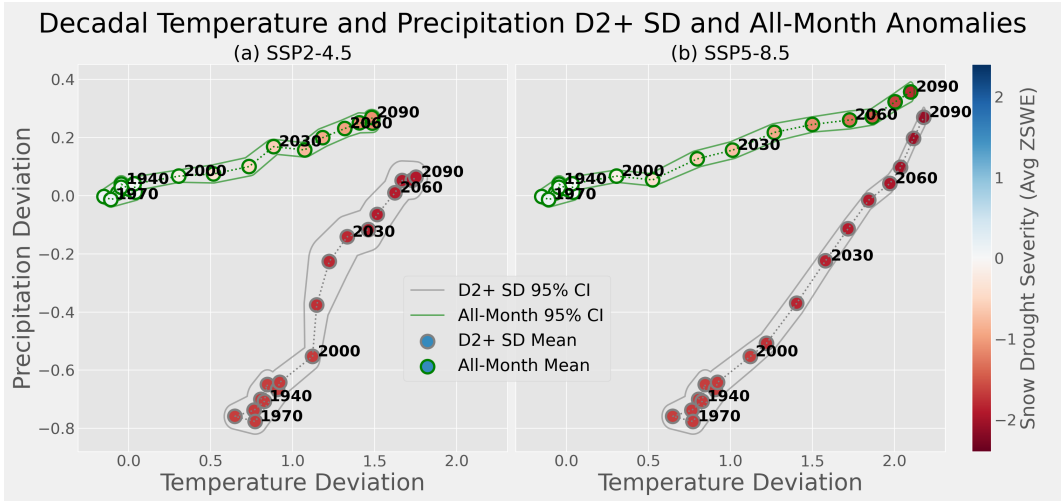


Figure 6. Temporal evolution of average temperature and precipitation anomalies with respect to the historical conditions (1921–2011). Each dot represents the average temperature and precipitation condition for historically snowy locations during winter (Oct–April) for a given decade either for all months and locations (outlined in green) or only for months classified as D2+ (outlined in gray). Each point is shaded by its average ZSWE score; thus because D2+ SD months are restricted to have a ZSWE of less than -1.3 , these points average snow drought conditions are less than -1.3 . Both all-month and D2+ SD-month points are surrounded by a contour which captures 95% of ensemble members. Panel (a) depicts these changes under SSP2-4.5 while (b) depicts changes under SSP5-8.5.

with an average temperature and precipitation anomaly of 0.6 to 0.8 and -0.6 to -0.8, respectively, indicating historical snow droughts are primarily driven by a near equal combination of both warm and dry conditions. This corresponds to a drought month on-average being both warmer and drier than 75% of months.

However, by 2050 the average drought has become both warmer and *wetter*; under SSP5-8.5 the temperature deviation increases to 1.84 and the precipitation deviation increases to -0.015, meaning that it no longer takes any deviation from normal historical precipitation to produce a drought. Furthermore, we conclude future D2+ snow drought conditions are driven by the increasingly high temperature average, which is warmer than 97% of historical conditions. By 2090, the average drought month has a temperature deviation of 2.18 and precipitation deviation of 0.27, very close to the all-month anomalies of 2.10 and 0.36 for temperature and precipitation, respectively; both the average monthly temperature for both D2+ and all-month averages are in the 98th percentile of historical conditions, indicating not only that future winter conditions will on average be extremely warm, but that the difference between average conditions for all months and drought months alone has narrowed significantly. Examining the ZSWE scores for 2090 under SSP5-8.5 confirms that the convergence is also reflected in SWE changes, with the average all-month ZSWE being -1.79 and the average D2+ month having a ZSWE of -2.10. Thus, the all-month average is expected to be an extreme drought, while the average drought is expected to be exceptional. Under SSP2-4.5, conditions do not become quite as extreme, with average all-month conditions by 2090 reaching 1.48 for temperature, 0.27 for precipitation, and -1.10 ZSWE. We note that although the gap to the D2+ condition (1.75, 0.064, and -1.91 for T, P, and ZSWE), narrows it is far less extreme than under SSP5-8.5; the average month is only given a D1 snow drought classification. The convergence of the all-month and D2+ temperature and precipitation anomalies,

389 particularly under SSP5-8.5 emphasize that D2+ SDs will require increasingly smaller
 390 deviations from normal conditions to produce. This underscores that snow droughts will
 391 become the dominant regime in the WUS by the end of the 21st century.

392 3.4 Timeline for Snow Free Conditions

393 In addition to changes in D2+ SD frequency, we also examine how total SWE avail-
 394 ability is expected to change, by assessing the timing of Western regions transition to
 395 a no-snow regime. A no-snow regime, characterized by a 10-year moving average of April
 396 snowpack consistently below 10% of the historical April average, is potentially catastrophic
 397 as it indicates severely limited summer water supply from snowpack. To understand when
 398 a no-snow regime is likely to affect an HUC2 region, we examine the distribution of trans-
 399 sition times to no-snow across SPEAR's ensemble members. By varying the area thresh-
 400 old, \mathcal{A} , we can assess how quickly conditions are expected to deteriorate. Figure 7 shows
 401 the distribution of the transition to no snow regimes for 3 different area thresholds, \mathcal{A} :
 402 50%, 75%, and 90%, for the historically snowy HUC2 regions. Note that by construc-
 403 tion, an individual ensemble member's transition year always occurs later for higher \mathcal{A} .
 404 However the ensemble distributions can overlap, which indicates large variability in the
 405 severity of conditions, especially later this century.

406 For $\mathcal{A} = 0.5$, we find that the historically snowy WUS, or "West-Wide", transi-
 407 tion time, averaged across all regions is 2071 for SSP2-4.5 and 2048 for SSP5-8.5. Across
 408 regions however, transition times varied from as early as 2025 (CA) to 2088 (UC) for SSP2-
 409 4.5 and 2018 (CA) to 2056 (UC) for SSP5-8.5. The snow-free transition distribution cen-
 410 ter occurs later for all regions under the SSP2-4.5 scenario when compared with SSP5-
 411 8.5. The scenario difference is less pronounced in regions which experience a no-snow trans-
 412 sition earlier, such as California. We conclude that while a lower emission scenario im-
 413 proves the probability that the transition to a no-snow regime occurs later, internal cli-
 414 mate variability could still result in periods of no snow much sooner than the ensemble
 415 mean predicts.

416 Another notable feature of Figure 7 is the large range of transition times within
 417 each region of the 30-ensemble member transition times. We find that in some ensem-
 418 ble members, the earliest transition occurs over 15 years earlier than the median tran-
 419 sition for many regions. For example, in the Lower Colorado region, the first ensemble
 420 member transitions to no-snow in 2069 while the mean transition time of the ensemble
 421 members isn't until 2086. Thus, while the LC is not likely to see these extreme condi-
 422 tions until the 2080s their hydrological infrastructure, snow tourism economies, and fire
 423 response must be prepared significantly earlier to face these conditions. The shape of the
 424 transition time distribution under SSP2-4.5 is also more spread out than the high emis-
 425 sion scenario indicating a larger uncertainty in the onset of no-snow conditions. This is
 426 consistent with our expectation that more rapid warming under SSP5-8.5 will acceler-
 427 ate the timeline associated with a transition to no-snow, the compressed timeline is sim-
 428 ply a byproduct of this effect. In other words, temperature and precipitation changes
 429 are happening more slowly in SSP2-4.5 which leads to internal climate variability being
 430 a more important factor in determining no-snow transition times, while in SSP5-8.5, the
 431 accelerated radiative forcing is the dominant effect. As a result, many regions under SSP2-
 432 4.5 experience transition times that occur before ensemble members under SSP5-8.5. For
 433 example, in the Pacific Northwest a quarter of the SSP2-4.5 realizations transitioned be-
 434 fore the median ensemble member under SSP5-8.5. This suggests that emission reduc-
 435 tions, while likely to improve the odds that a no-snow transition occurs later in the cen-
 436 tury, do not guarantee a latter arrival of these conditions. This is particularly true for
 437 regions where the transition is projected to occur earlier in the century, likely because
 438 scenario forcing is much more similar.

439 To assess the probability that a region becomes snow free over the next century,
 440 we examine the fraction of ensemble members that transition to no-snow before 2100.
 441 We model the likelihood of the transition by the maximum likelihood estimator (MLE),

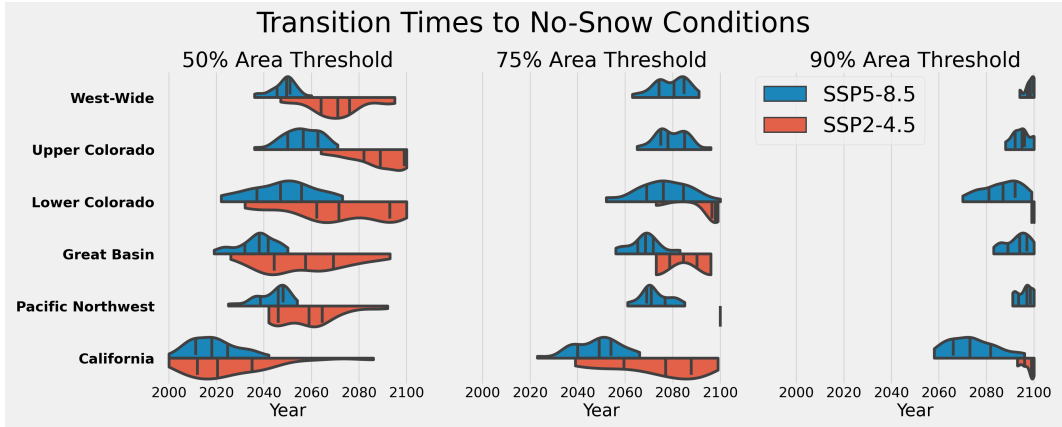


Figure 7. Distribution of SPEAR-simulated transition times to no snow regimes, or \mathcal{T} , by Western HUC2 region, split between SSP5-8.5 and SSP2-4.5 scenarios. The 3 subplots represent the different thresholds \mathcal{A} . Meeting a higher threshold corresponds with an increased proportion of the region experiencing perennial no-snow conditions, and implies more severe conditions. The vertical lines in the distributions represent the quantiles of the ensemble members that transition. We also include a transition time for the entire historically snowy WUS, labeling it “West-Wide.

or fraction of ensemble members that hit the transition threshold by 2100, and display these values in Table 8. By further splitting across the low and high emission scenarios, we can model how the risk also changes as a function of the radiative forcing scenario. In Table 8b, we see that under SSP5-8.5, $\mathcal{A} = 0.75$ is guaranteed by 2100 across all regions. The highest threshold, $\mathcal{A} = 0.9$ is guaranteed only for California, while uncertainty remains for the other 4 HUC2s. Conditions by 2100 are much less severe under SSP2-4.5, with only $\mathcal{A} = 0.5$ likely or certain for all regions, while for $\mathcal{A} = 0.75$, only California is very likely to transition to a low snow regime; the other regions have low probability of doing so. For $\mathcal{A} = 0.9$ it is unlikely that any region will have transitioned by 2100 under SSP2-4.5.

Furthermore, when we compare the order of how likely regions are to transition to no-snow conditions with the regions average historical temperature, we find the coldest regions are in general least likely to transition while the warmest are most likely. For example, under SSP5-8.5 with $\mathcal{A} = 90\%$, the region ordering by temperature and transition probability is the same: UC (-5.1°C, 30%), PNW (-3.9°C, 53%), GB (-2.4°C, 70%), LC (-0.7°C, 83%), and CA (0.3°C, 100%). This finding emphasizes the role mean winter temperature plays in dictating a region’s no-snow transition probability. Like Shrestha et al. (2021) we find that warming any region with a winter average of $> -5^\circ\text{C}$, negatively impacts snowpack.

Table 8 indicates that under either SSP2-4.5 or SSP5-8.5 we expect at least half of the historically snowy WUS to have less than 10% of its historical April snowpack by 2100. Both columns where $\mathcal{A} = 50\%$ show greater than 80% probability for all regions, with the threshold guaranteed under SSP5-8.5. We also find that under SSP5-8.5, 4 of the 5 Western watersheds are more likely than not to cross the $\mathcal{A} = 90\%$ no-snow threshold by 2100. Upper Colorado is the exception with only a 30% chance, likely driven by its colder average winter temperatures. While these numbers are shocking, it’s important to consider how snow-covered area and total snow volume differ. As snowpack declines are dominated by losses at lower elevations that are closer to the freezing point, we expect that the extreme loss of snow-covered area predicted by SPEAR will overestimate the amount of total winter water storage lost, since the higher elevations typi-

Probability of No-Snow Transition by 2100

| Region | SSP2-4.5 | | | SSP5-8.5 | | |
|-------------------|----------|-----|-----|----------|-----|-----|
| | 50% | 75% | 90% | 50% | 75% | 90% |
| Upper Colorado | 83 | 0 | 0 | 100 | 97 | 30 |
| Lower Colorado | 87 | 23 | 7 | 100 | 100 | 83 |
| Great Basin | 100 | 7 | 0 | 100 | 100 | 70 |
| Pacific Northwest | 100 | 3 | 0 | 100 | 100 | 53 |
| California | 100 | 93 | 17 | 100 | 100 | 100 |
| West-Wide | 100 | 0 | 0 | 100 | 100 | 20 |

Figure 8. Probability of a snow free transition occurring before 2100 at the 3 thresholds \mathcal{A} based on the fraction of ensemble members who transition to a no-snow regime by 2100. We show the probabilities by area threshold, 50%, 75%, and 90%, across SSP2-4.5 and SSP5-8.5 for the historically snowy portions of each of the 5 Western HUC2 regions.

cally store the most snowpack (Mote et al., 2005; Minder, 2009). Therefore we expect the area-based no-snow transition to over-predict the hydrological impact of warming.

4 Remarks

According to SPEAR, widespread increases in D2+ SDs have already been observed in the historical period, which estimates the WUS D2+ SD frequency has increased by 43%, with an average 95% confidence interval of 22 to 65%. These findings are slightly higher, although still consistent with, Huning and AghaKouchak (2020) whose slightly different time period found a 28% increase in D2+ SD frequency for the WUS over 1980-2018. SPEAR predicts even more dramatic changes heading into the 21st century, classifying over 35% of winter months as snow droughts under RCP2-4.5 and 60% under RCP5-8.5 by 2100, compared with a normalized 9.6% across the historical period. These changes were found to be primarily driven by increasing temperatures, which on average exceeded the 93rd and 97th percentile (2 standard deviations) of historical temperature records by 2100 under RCP2-4.5 and RCP4-8.5, respectively. We also found that across all regions, the transition to a no-snow regime, where over 90% of the historically snowy region had on average less than 10% of the April historical maximum, was more likely than not in 4 out of the 5 HUC2s studied under RCP5-8.5, the UC region being the exception. Under RCP2-4.5, only the 50% threshold was very likely for all regions, emphasizing the role that emissions this century will play in determining no-snow transition.

491 Similar to Shrestha et al. (2021), who found a strong correlation between decreasing
 492 latitude and decreased snowpack. We find the probability of a no-snow transition is
 493 much more likely for regions which have higher average winter temperatures. In partic-
 494 ular, the Lower Colorado and California Regions, which are the most southern, had the
 495 highest probabilities of reaching no-snow conditions across both emissions scenarios and
 496 all area threshold values, and similarly had historical winter temperatures averaging near
 497 0°C. The Pacific Northwest and Upper Colorado, the coldest regions on average, typi-
 498 cally had the smallest transition probabilities.

499 While using a GCM allows us to examine multiple realizations of the climate to
 500 derive these probabilities, it is inherently limited by the model assumption constraints.
 501 In particular, the large resolution of a 1/2° global climate model is unable to resolve com-
 502 plex mountain topography and can result in significant warm biases which predicts less
 503 snow at elevation, as shown by Matiu and Hanzer (2022). We expect this may make SPEAR
 504 snowpack estimates particularly sensitive to warming, and therefore likely to overesti-
 505 mate increases in snow drought. Another recent paper from Hoylman et al. (2022) as-
 506 serts that using timescales longer than 30 years, as has been done in the vast majority
 507 of previous literature (Svoboda et al., 2002), as the baseline climatology can result in over-
 508 estimating the drought threat. Further work should be done to investigate the effect of
 509 the reference window on drought severity estimation.

510 Here, we've assessed changes in snow drought frequency, focusing on how the un-
 511 derlying climatology is expected to change, alongside modeling the distribution of ex-
 512 pected no-snow transition times. This study has implications for Western hydrology and
 513 snow tourism which is expected to see losses of 50% of ski season length by 2050 and 80%
 514 by 2090 (Wobus et al., 2017). One promising avenue for future research is to examine
 515 snow drought frequency changes over smaller regions, such as HUC4 regions to tease out
 516 which sub-regions are most vulnerable. This would also allow us to further examine lat-
 517 itude and elevation dependence. Also, estimating total SWE losses and melt timing across
 518 each region would allow us to better estimate the impacts of snow droughts on the West's
 519 hydrological system. The impacts of future snow droughts will be felt across the entire
 520 country, both directly from the hydrological or tourism resources that consistent snow-
 521 pack provides, and indirectly through loss of agricultural output from summer water short-
 522 ages or drifting wildfire smoke and warrant further investigations. Understanding the
 523 probable severity and timing of when these conditions are supposed to become most dam-
 524 aging, alongside both emissions uncertainty and uncertainty derived from internal cli-
 525 mate variability, will allow policymakers and infrastructure planners to best prepare the
 526 West for a future with less snow.

527 Acknowledgments

528 Many thanks to Sarah Kapnick for helping to inspire this project. We would also like
 529 to thank the NOAA Hollings Scholarship Program for funding this research.

530 References

- 531 Barnett, T. P., Adam, J. C., & Lettenmaier, D. P. (2005, November). Potential
 532 impacts of a warming climate on water availability in snow-dominated re-
 533 gions. *Nature*, 438(7066), 303–309. Retrieved 2022-07-26, from <https://www.nature.com/articles/nature04141> (Number: 7066 Publisher: Nature
 534 Publishing Group) doi: 10.1038/nature04141
- 535 Delworth, T. L., Cooke, W. F., Adcroft, A., Bushuk, M., Chen, J.-H., Dunne,
 536 K. A., ... Zhao, M. (2020). Spear: The next generation gfdl modeling
 537 system for seasonal to multidecadal prediction and projection. *Journal of
 538 Advances in Modeling Earth Systems*, 12(3), e2019MS001895. Retrieved
 539 from <https://agupubs.onlinelibrary.wiley.com/doi/abs/10.1029/2019MS001895> (e2019MS001895 2019MS001895) doi: <https://doi.org/10.1029/2019MS001895>

- 542 2019MS001895
- 543 Deser, C., Lehner, F., Rodgers, K. B., Ault, T., Delworth, T. L., DiNezio, P. N., ...
 544 Ting, M. (2020, April). Insights from earth system model initial-condition
 545 large ensembles and future prospects. , 10(4), 277–286. Retrieved 2022-08-31,
 546 from <https://www.nature.com/articles/s41558-020-0731-2> (Number: 4
 547 Publisher: Nature Publishing Group) doi: 10.1038/s41558-020-0731-2
- 548 Gergel, D. R., Nijssen, B., Abatzoglou, J. T., Lettenmaier, D. P., & Stumbaugh,
 549 M. R. (2017). Effects of climate change on snowpack and fire potential in the
 550 western USA. , 141(2), 287–299. Retrieved from <https://doi.org/10.1007/s10584-017-1899-y> doi: 10.1007/s10584-017-1899-y
- 552 Harpold, A., Dettinger, M., & Rajagopal, S. (2017, 02). Defining snow drought and
 553 why it matters. *Eos Transactions American Geophysical Union*. doi: 10.1029/
 554 2017EO068775
- 555 Hoylman, Z. H., Bocinsky, R. K., & Jencso, K. G. (2022). Drought assessment has
 556 been outpaced by climate change: empirical arguments for a paradigm shift. ,
 557 13(1), 2715. Retrieved 2022-11-12, from <https://www.nature.com/articles/s41467-022-30316-5> (Number: 1 Publisher: Nature Publishing Group) doi:
 559 10.1038/s41467-022-30316-5
- 560 Huning, L. S., & AghaKouchak, A. (2020). Global snow drought hot spots and
 561 characteristics. *Proceedings of the National Academy of Sciences*, 117(33),
 562 19753–19759. Retrieved from <https://www.pnas.org/doi/abs/10.1073/pnas.1915921117> doi: 10.1073/pnas.1915921117
- 564 Kim, R. S., Kumar, S., Vuyovich, C., Houser, P., Lundquist, J., Mudryk, L.,
 565 ... Wang, S. (2021). Snow ensemble uncertainty project (seup): quantification of snow water equivalent uncertainty across north america via
 566 ensemble land surface modeling. *The Cryosphere*, 15(2), 771–791. Retrieved
 568 from <https://tc.copernicus.org/articles/15/771/2021/> doi:
 569 10.5194/tc-15-771-2021
- 570 Livneh, B., Rosenberg, E. A., Lin, C., Nijssen, B., Mishra, V., Andreadis, K. M.,
 571 ... Lettenmaier, D. P. (2013). A long-term hydrologically based dataset
 572 of land surface fluxes and states for the conterminous united states: Update and extensions. *Journal of Climate*, 26(23), 9384 - 9392. Retrieved
 573 from <https://journals.ametsoc.org/view/journals/clim/26/23/jcli-d-12-00508.1.xml> doi: 10.1175/JCLI-D-12-00508.1
- 576 Maher, N., Kay, J. E., & Capotondi, A. (2022). Modulation of ENSO teleconnections over north america by the pacific decadal oscillation. , 17(11), 114005.
 577 Retrieved 2022-11-01, from <https://dx.doi.org/10.1088/1748-9326/ac9327>
 579 (Publisher: IOP Publishing) doi: 10.1088/1748-9326/ac9327
- 580 Matiu, M., & Hanzer, F. (2022). Bias adjustment and downscaling of snow cover
 581 fraction projections from regional climate models using remote sensing for the
 582 european alps. *Hydrology and Earth System Sciences*, 26(12), 3037–3054. Retrieved
 583 from <https://hess.copernicus.org/articles/26/3037/2022/> doi:
 584 10.5194/hess-26-3037-2022
- 585 McCrary, R. R., McGinnis, S., & Mearns, L. O. (2017). Evaluation of snow
 586 water equivalent in narccap simulations, including measures of observational uncertainty. *Journal of Hydrometeorology*, 18(9), 2425 - 2452. Retrieved
 588 from https://journals.ametsoc.org/view/journals/hydr/18/9/jhm-d-16-0264_1.xml doi: 10.1175/JHM-D-16-0264.1
- 590 McCrary, R. R., Mearns, L. O., Hughes, M., Biner, S., & Bukovsky, M. S. (2022,
 591 February). Projections of North American snow from NA-CORDEX and their
 592 uncertainties, with a focus on model resolution. *Climatic Change*, 170(3), 1-25.
 593 Retrieved from https://ideas.repec.org/a/spr/climat/v170y2022i3d10007_s10584-021-03294-8.html doi: 10.1007/s10584-021-03294-8
- 595 Minder, J. R. (2009). The sensitivity of mountain snowpack accumulation to climate
 596 warming. *Journal of Climate*, 23, 2634 - 2650.

- 597 Mote, P. W., Hamlet, A. F., Clark, M. P., & Lettenmaier, D. P. (2005). Declining
598 mountain snowpack in western north america*. *Bulletin of the American Mete-*
599 *orological Society*, 86(1), 39 - 50. Retrieved from <https://journals.ametsoc.org/view/journals/bams/86/1/bams-86-1-39.xml> doi: 10.1175/BAMS-86
600 -1-39
- 601 Shrestha, R. R., Bonsal, B. R., Bonnyman, J. M., Cannon, A. J., & Najafi, M. R.
602 (2021). Heterogeneous snowpack response and snow drought occurrence across
603 river basins of northwestern north america under 1.0 °c to 4.0 °c global warm-
604 ing. *Climatic Change*, 164(3), 40.
- 605 Siirila-Woodburn, E. R., Rhoades, A. M., Hatchett, B. J., Huning, L. S., Szinai, J.,
606 Tague, C., ... Kaatz, L. (2021). A low-to-no snow future and its impacts
607 on water resources in the western united states. *Nature Reviews Earth &*
608 *Environment*, 2(11), 800–819. Retrieved from <https://doi.org/10.1038/s43017-021-00219-y> doi: 10.1038/s43017-021-00219-y
- 609 Svoboda, M., LeComte, D., Hayes, M., Heim, R., Gleason, K., Angel, J., ...
610 Stephens, S. (2002). The drought monitor. *Bulletin of the American Me-*
611 *teorological Society*, 83(8), 1181 - 1190. Retrieved from https://journals.ametsoc.org/view/journals/bams/83/8/1520-0477-83_8_1181.xml doi:
612 10.1175/1520-0477-83.8.1181
- 613 Trujillo, E., Molotch, N. P., Goulden, M. L., Kelly, A. E., & Bales, R. C. (2012).
614 Elevation-dependent influence of snow accumulation on forest greening. ,
615 5(10), 705–709. Retrieved 2022-07-26, from <https://www.nature.com/articles/ngeo1571> (Number: 10 Publisher: Nature Publishing Group)
616 doi: 10.1038/ngeo1571
- 617 Wobus, C., Small, E. E., Hosterman, H., Mills, D., Stein, J., Rissing, M., ... Mar-
618 tinich, J. (2017). Projected climate change impacts on skiing and snowmobil-
619 ing: A case study of the united states. *Global Environmental Change*, 45, 1-14.
620 Retrieved from <https://www.sciencedirect.com/science/article/pii/S0959378016305556> doi: <https://doi.org/10.1016/j.gloenvcha.2017.04.006>
- 621 Wrzesien, M. L., Pavelsky, T. M., Durand, M. T., Dozier, J., & Lundquist, J. D.
622 (2019). Characterizing biases in mountain snow accumulation from global data
623 sets. *Water Resources Research*, 55(11), 9873-9891. Retrieved from <https://agupubs.onlinelibrary.wiley.com/doi/abs/10.1029/2019WR025350> doi:
624 <https://doi.org/10.1029/2019WR025350>
- 625
- 626
- 627
- 628
- 629
- 630